# Electronic Supplementary Information

# Conversion of High-Spin Iron(III)-Alkylperoxo to Iron(IV)-Oxo Species via O-O Bond Homolysis in Nonheme Iron Models

Seungwoo Hong,[†ab] Yong-Min Lee,[†a] Kyung-Bin Cho,[a] Mi Sook Seo,[a] Dayoung Song,[a] Jihae Yoon,[a] Ricardo Garcia-Serres,[c] Martin Clémancey,[d] Takashi Ogura,[e] Woonsup Shin,*[b] Jean-Marc Latour,*[f] and Wonwoo Nam*[a]

[a]*Department of Chemistry and Nano Science, Department of Bioinspired Science, Ewha Womans University, Seoul 120-750, Korea,*

[b]*Department of Chemistry and Interdisciplinary Program of Integrated Biotechnology, Sogang University, Seoul 121-742, Korea*

[c]*University of Grenoble Alpes, LCBM, F-38054 Grenoble, France*

[d]*CNRS UMR 5249, LCBM, F-38054 Grenoble, France*

[e]*Picobiology Institute, Graduate School of Life Science, University of Hyogo, Hyogo 678-1297, Japan*

[f]*CEA, DSV, iRTSV, LCBM, PMB, F-38054 Grenoble, France*

E-mail: shinws@sogang.ac.kr (W.S.), jean-marc.latour@cea.fr (J.M.L.), wwnam@ewha.ac.kr (W.N.)

[†]These authors contributed equally to this work.

# Table of Contents

## Experimental Section

**Materials**. All chemicals obtained from Aldrich Chemical Co. were the best available purity and used without further purification unless otherwise indicated. Solvents were dried according to published procedures and distilled under Ar prior to use.[S1] $H_2{}^{18}O$ (95% $^{18}O$-enriched) and $^{18}O_2$ (70% enriched) were purchased from ICON Services Inc. (Summit, NJ, USA). Doubly labeled cumyl$^{18}O^{18}OH$ (70% $^{18}O$-enriched) was synthesized by reacting cumene and $^{18}O_2$ in hexane at 85 °C according to the procedure of Finn and Sharpless.[S2] $Fe(CF_3SO_3)_2{\cdot}2CH_3CN$ was synthesized by reacting iron powder with trifluoromethane-sulfonic acid ($CF_3SO_3H$) under inert atmosphere in $CH_3CN$. $[Fe(13\text{-}TMC)(CF_3SO_3)](CF_3SO_3)$ and $[Fe^{IV}(O)(13\text{-}TMC)]^{2+}$ were synthesized according to literature methods.[S3]

**Instrumentation**. UV-vis spectra were recorded on a Hewlett Packard Agilent 8453 UV-visible spectrophotometer equipped with a circulating water bath or an UNISOKU cryostat system (USP-203; UNISOKU, Japan) or on a Hi-Tech Scientific (U.K.) SF-61 DX2 cryogenic stopped-flow spectrometer equipped with a Xe arc lamp and a KinetaScan diode array rapid scanning unit. Electrospray ionization mass (ESI MS) spectra were collected on a Thermo Finnigan (San Jose, CA, USA) LCQ$^{TM}$ Advantage MAX quadrupole ion trap instrument, by infusing samples directly into the source at 20 μL/min using a syringe pump. The spray voltage was set at 4.7 kV and the capillary temperature at 80 °C. CW-EPR spectra were taken at 5.0 K using a X-band Bruker EMX-plus spectrometer equipped with a dual mode cavity (ER 4116DM). Low temperatures were achieved and controlled with an Oxford Instruments ESR900 liquid He quartz cryostat with an Oxford Instruments ITC503 temperature and gas flow controller. $^1$H NMR spectra were measured with Bruker DPX-400 spectrometer. Resonance Raman spectra were obtained using a liquid nitrogen cooled CCD detector (CCD-1024x256-OPEN-1LS, HORIBA Jobin Yvon) attached to a 1-m single polychromator (MC-100DG, Ritsu Oyo Kogaku) with a 1200 grooves/mm holographic grating. Excitation wavelengths of 407.0 nm and 441.6 nm were provided by He-Cd laser (Kimmon Koha, IK5651R-G and KR1801C), with 20 mW power at the sample point. All measurements were carried out with a spinning cell (1000 rpm) at –20 °C. Raman shifts were calibrated with indene, and the accuracy of the peak positions of the Raman bands was ± 1 $cm^{-1}$. The isomer shifts are referenced against that of a room-temperature metallic iron foil. Analysis of the data was performed with the program WMOSS (WEB Research).

**Mössbauer Analysis.** Mössbauer spectra were recorded at 4.2 K and 80 K, either on a lowfield Mössbauer spectrometer equipped with a Janis SVT-400 cryostat or on a strong-field Mössbauer spectrometer equipped with an Oxford Instruments Spectromag 4000 cryostat containing an 8T split-pair superconducting magnet. Both spectrometers were operated in a constant acceleration mode in transmission geometry. The isomer shifts are referenced against that of a room-temperature metallic iron foil. Analysis of the data was performed with the program WMOSS (WEB Research). The majority species in spectrum E (pink) is assigned to $^{BH}$**2** based on the similarity of their parameters, although these are not completely identical. An alternate assignment would be that it represents $^{BH}$**2-NCS**, the orange component being an impurity formed by substitution of the peroxo moiety.

**Generation and Characterization of [Fe$^{III}$(OOC(CH$_3$)$_3$)(13-TMC)]$^{2+}$ ($^{BH}$2) and [Fe$^{III}$(OOC(CH$_3$)$_2$C$_6$H$_5$)(13-TMC)]$^{2+}$ ($^{CH}$2).** The intermediates, $^{BH}$**2** and $^{CH}$**2**, were prepared by treating the solution of [Fe(13-TMC)(CF$_3$SO$_3$)](CF$_3$SO$_3$) (**1**: 0.50 mM) with 3 equiv. of *tert*-butyl hydroperoxide (*t*-BuOOH) and 3 equiv. of cumyl hydroperoxide (CumylOOH) in CH$_3$CN at –40 °C, respectively. The formation of $^{BH}$**2** and $^{CH}$**2** was followed by monitoring UV-vis spectral changes of the reaction solutions at 510 nm and 500 nm, respectively. The electron paramagnetic resonance (EPR) spectra of $^{BH}$**2** and $^{CH}$**2** (1.0 mM) were recorded at 5.0 K. The *g* values of $^{BH}$**2** and $^{CH}$**2** indicated the high-spin state of both intermediates. Resonance Raman (rRaman) spectroscopic measurements were performed with $^{CH}$**2** and $^{18}$O-labeled $^{CH}$**2** intermediates, [Fe$^{III}$($^{16}$O$^{16}$OC(CH$_3$)$_2$C$_6$H$_5$)(13-TMC)]$^{2+}$ and [Fe$^{III}$($^{18}$O$^{18}$OC(CH$_3$)$_2$C$_6$H$_5$)(13-TMC)]$^{2+}$, which were generated by adding 3 equiv. of Cumyl$^{16}$O$^{16}$OH and Cumyl$^{18}$O$^{18}$OH (70% $^{18}$O-enriched) to a solution of **1** (16 mM) in CH$_3$CN at –40 °C, respectively. Upon excitation of laser wavelength at 442 nm, the isotopic Raman bands shifts were observed by comparing the Raman bands of $^{CH}$**2** and $^{18}$O-labeled $^{CH}$**2**.

**Generation and Characterization of [Fe$^{IV}$(O)(13-TMC)(NCS)]$^{+}$ (4).** The intermediate **4** was prepared by treating **1** (0.50 mM) with 3 equiv. of iodosylbenzene (PhIO), followed by a subsequent addition of 1.2 equiv. of sodium thiocyanate (NaNCS) to the resulting solution in CH$_3$CN at –40 °C. The formation of **4** was followed by monitoring UV-vis spectral changes of the reaction solutions at 755 nm. rRaman and ESI MS spectral measurements were performed to characterize **4**. The $^{16}$O-labeled and $^{18}$O-labeled **4**, [Fe$^{IV}$($^{16}$O)(13-TMC)(NCS)]$^{+}$ and [Fe$^{IV}$($^{18}$O)(13-TMC)(NCS)]$^{+}$, were obtained by adding 1.2 equiv. of NaNCS to the

reaction solution containing $[Fe^{IV}(^{16}O)(13\text{-TMC})]^{2+}$ and $[Fe^{IV}(^{18}O)(13\text{-TMC})]^{2+}$ in $CH_3CN$ at –40 °C, respectively. Upon 407-nm excitation, an isotopic shift of resonance-enhanced vibration was observed (Fig. 4c). In ESI MS spectrum, the mass-to-charge ratio (*m/z*) of 372.1 and 374.2 and their isotopic distribution patterns corresponding to $[Fe^{IV}(^{16}O)(13\text{-TMC})(NCS)]^{+}$ and $[Fe^{IV}(^{18}O)(13\text{-TMC})(NCS)]^{+}$, respectively, were observed (Fig. 4b).

**Conversion of $[Fe^{III}(OOR)(13\text{-TMC})]^{2+}$ ($^{CH}$2 and $^{BH}$2) to 4 upon Addition of $NCS^{-}$.** All reactions were followed by monitoring UV-vis spectral changes of reaction solutions with a Hewlett Packard 8453 spectrophotometer equipped with cryostat system or a Hi-Tech Scientific SF-61 DX2 cryogenic stopped-flow spectrophotometer. The conversion of $[Fe^{III}(OOR)(13\text{-TMC})]^{2+}$ ($^{CH}$**2** and $^{BH}$**2**) to **4** was carried out by adding 1.2 equiv. of NaNCS to the solution of $[Fe^{III}(OOR)(13\text{-TMC})]^{2+}$ (0.50 mM) in $CH_3CN$ at –40 °C. The conversion was examined by monitoring the decrease of absorption band at 510 nm due to $^{BH}$**2** or 500 nm due to $^{CH}$**2** and concomitant increase at 755 nm due to **4**. The conversion of $^{BH}$**2** (final concentration of 0.50 mM) to **4**, monitored with a stopped-flow spectrophotometer, was carried out by mixing the solutions of NaNCS (1.2 equiv.) and $^{BH}$**2** in the push of a single-mixing experiment in $CH_3CN$ at –40 °C. All reactions were collected using a 1.0 cm optical path length at the given temperature. The raw kinetic data were treated with KinetAsyst 3 (Hi-Tech Scientific) and Specfit/32 Global Analysis System software from Spectrum Software Associates. Reactions were run at least in triplicate, and data reported represent the average of these reactions.

**X-ray Structural Analysis**. Single crystals of $[Fe^{II}(13\text{-TMC})(NCS)](CF_3SO_3)$ were grown by slow diffusion of ether into an acetonitrile solution and mounted on a glass fiber tip with epoxy cement. The diffraction data for $[Fe^{II}(13\text{-TMC})(NCS)](CF_3SO_3)$ were collected at 120 K on a Bruker SMART AXS diffractometer equipped with a monochromator in the Mo Kα (λ = 0.71073 Å) incident beam. The CCD data were integrated and scaled using the Bruker-SAINT software package, and the structure was solved and refined using SHEXTL V 6.12.[S4] Hydrogen atoms were located in the calculated positions. Crystal data for $[Fe^{II}(13\text{-TMC})(NCS)](CF_3SO_3)$: $C_{19}F_3FeN_7O_3S_2$, *Orthorhombic*, *Pnma*, $Z = 4$, $a = 24.2856(5)$, $b = 12.7122(3)$, $c = 9.1833(2)$ Å, $\alpha = 90$, $\beta = 90$, $\gamma = 90°$, $V = 2835.10(11)$ Å$^3$, $\mu = 0.728$ mm$^{-1}$, $d_{calc} = 1.291$ g/cm$^3$, $R_1 = 0.0680$, $wR_2 = 0.2209$ for 3348 unique reflections, 244 variables. The crystallographic data for $[Fe^{II}(13\text{-TMC})(NCS)](CF_3SO_3)$ are summarised in Table S2,

and the selected bond distances and angles are listed in Table S3. CCDC 959085 contains the supplementary crystallographic data for this paper. These data can be obtained free of charge via www.ccdc.cam.ac.uk/data_request/cif (or from the Cambridge Crystallographic Data Centre, 12, Union Road, Cambridge CB2 1EZ, UK; fax: (+44) 1223-336-033; or deposit@ccdc.cam.ac.uk).

**EPR Measurements for the Conversion of $^{BH}$2 to 4.** EPR measurements for the conversion reaction of $^{BH}$**2** to **4** was performed as follows: The reaction solution was prepared by adding NaNCS (0.60 mM) to a solution of $^{BH}$**2** (0.50 mM). The EPR samples of the reaction solution were taken at the time indicated in Fig. 5c footnote. X-band EPR spectra were recorded at 5.0 K. The experimental parameters for EPR spectra were as follows: Microwave frequency = 9.646GHz, microwave power = 1.0 mW, modulation amplitude = 10 G, gain = 1.0 x $10^4$, modulation frequency = 100 kHz, time constant = 81.92 ms, and conversion time = 81.00 ms.

**Titration Experiment for the Conversion of $^{BH}$2 to 4.** The conversion of $^{BH}$**2** to **4** was titrated by adding incremental amounts of NaNCS (0.20, 0.40, 0.60, 0.80, 1.0, and 1.2 equiv.) to the solution of $^{BH}$**2** (0.50 mM) in $CH_3CN$ at –40°C. The titration data were obtained by monitoring UV-vis spectral changes at 510 nm due to $^{BH}$**2** and 755 nm due to **4**.

**Product Analysis.** Products formed in the reaction of $^{CH}$**2** (0.50 mM) and NaNCS (0.60 mM) in $CH_3CN$ at –40 °C were analyzed by High Performance Liquid Chromatography (HPLC, DIOMEX Pump Series P580) equipped with a variable wavelength UV-200 detector. Quantitative analysis was made on the basis of comparison of HPLC peak integration between products and authentic samples. In the conversion of $^{CH}$**2** to **4**, acetophenone was formed as the sole product with more than 80% yield.

**DFT Methods**. DFT calculations were performed with Gaussian 09 package[S5] at B3LYP/LACVP//LACV3P$^{*+}$ level,[S6] with the sulfur atom requiring 6-311+G$^*$//6-311+G(3df). Long range solvent effect was included using the CPCM scheme[S7] as implemented in Gaussian, and was included during the optimizations as well. The energies quoted in the text are electronic energies evaluated using sigle point large basis sets. Although the free energies have been evaluated (see Table S4), frequency calculations on solvent optimized structures introduce a formal error due to the parametrical nature of the CPCM scheme.[S8] Albeit this

error is not expected to affect the free energies in any significant manner in the current particular case, we present the free energies only in the SI.

**References**

S1. W. L. F. Armarego, C. L. L. Chai, *Purification of Laboratory Chemicals*. 6th edn, Pergamon Press, Oxford, U.K. 2009.

S2. M. G. Finn and K. Barry Sharpless, *J. Am. Chem. Soc.,* 1991, **113**, 113-126

S3. S. Hong, H. So, H. Yoon, K.-B. Cho, Y.-M. Lee, S. Fukuzumi and W. Nam, *Dalton Trans*., 2013, **42**, 7842-7845.

S4. G. M. Sheldrick, *SHELXTL/PC Version 6.12 for Windows XP*, Bruker AXS Inc., Madison, Wisconsin, USA, **2001**.

S5**.** M. J. Frisch, G. W. Trucks, H. B. Schlegel, G. E. Scuseria, M. A. Robb, J. R. Cheeseman, G. Scalmani, V. Barone, B. Mennucci, G. A. Petersson, H. Nakatsuji, M. Caricato, X. Li, H. P. Hratchian, A. F. Izmaylov, J. Bloino, G. Zheng, J. L. Sonnenberg, M. Hada, M. Ehara, K. Toyota, R. Fukuda, J. Hasegawa, M. Ishida, T. Nakajima, Y. Honda, O. Kitao, H. Nakai, T. Vreven, J. A. Montgomery, Jr., J. E. Peralta, F. Ogliaro, M. Bearpark, J. J. Heyd, E. Brothers, K. N. Kudin, V. N. Staroverov, R. Kobayashi, J. Normand, K. Raghavachari, A. Rendell, J. C. Burant, S. S. Iyengar, J. Tomasi, M. Cossi, N. Rega, J. M. Millam, M. Klene, J. E. Knox, J. B. Cross, V. Bakken, C. Adamo, J. Jaramillo, R. Gomperts, R. E. Stratmann, O. Yazyev, A. J. Austin, R. Cammi, C. Pomelli, J. W. Ochterski, R. L. Martin, K. Morokuma, V. G. Zakrzewski, G. A. Voth, P. Salvador, J. J. Dannenberg, S. Dapprich, A. D. Daniels, Ö. Farkas, J. B. Foresman, J. V. Ortiz, J. Cioslowski and D. J. Fox, *Gaussian 09, Revision B.01 and D.01*, Gaussian, Inc., Wallingford CT, 2009.

S6. (a) A. D. Becke, *Phys. Rev. A,* 1988, **38**, 3098-3100. (b) A. D. Becke, *J. Chem. Phys.,* 1993, **98**, 1372. (c) A. D. Becke, *J. Chem. Phys.,* 1993, **98**, 5648. (d) C. Lee, W. Yang and R. G. Parr, *Phys. Rev. B,* 1988, **37**, 785-789. (e) P. J. Hay and W. R. Wadt, *J. Chem. Phys.,* 1985, **82**, 299. (f) K. G. Dyall, *Theor. Chem. Acc.,* 2004, **112**, 403-409.

S7. (a) V. Barone and M. Cossi, *J. Phys. Chem. A*, 1998, **102**, 1995-2001. (b) M. Cossi, N. Rega, G. Scalmani and V. Barone, *J. Comput. Chem.*, 2003, **24**, 669-681.

S8. J. Ho, A. Klamt and M. L. Coote, *J. Phys. Chem. A,* 2010, **114**, 13442-13444.

S9. J.-U. Rohde, J.-H. In, M. H. Lim, W. W. Brennessel, M. R. Bukowski, A. Stubna, E. Münck, W. Nam and L. Que, Jr, *Science*, 2003, **299**, 1037-1039

**Table S1**. Mössbauer and spin-Hamiltonian parameters used in the simulations. Data collected in acetonitrile frozen solution at 4.2 K.

| | (**1**) | (**2**) | (**3**) major | (**3**) minor | (**4**) |
|---|---|---|---|---|---|
| S | 2 | 5/2 | 5/2 | 5/2 | 1 |
| D, $cm^{-1}$ | | 6.5 | 13 | -0.17 | 28 [b] |
| E/D | | 0.06 | 0.09 | 0.01 | 0 [b] |
| $g_x,g_y,g_z$ | | 2.0, 2.0, 2.0 [a] | 2.0, 2.0, 2.0 [a] | 2.0, 2.0, 2.0 [a] | 2.3, 2.3, 2.0 [b] |
| $A_{x,y,z}/g_N\beta_N$, T | | -20.5 [c] | -21.3 [c] | -20.6 [c] | -24, -24 [d], -5 [a] |
| δ, mm/s | 1.00 | 0.32 | 0.29 | 0.45 | 0.07 |
| $\Delta E_Q$, mm/s | 3.87 | -0.44 | -0.59 | -0.71 | 1.34 |
| η | | 0 | 0 | 0.48 | 0 |

[a] fixed. [b] fixed, from ref.[S9] $A_x=A_y=A_z$ fixed. [d] $A_x=A_y$ fixed.

**Table S2**. Crystal data and structure refinement for $[Fe^{II}(13\text{-TMC})(NCS)](CF_3SO_3)$

| | |
|---|---|
| Empirical formula | $C_{19}F_3FeN_7O_3S_2$ |
| Formula weight | 551.23 |
| Temperature (K) | 170 |
| Wavelength (Å) | 0.71073 |
| Crystal system/space group | Orthorhombic, *Pnma* |
| Unit cell dimensions | |
| *a* (Å) | 24.2856(5) |
| *b* (Å) | 12.7122(3) |
| *c* (Å) | 9.1833(2) |
| $\alpha$ (°) | 90.00 |
| $\beta$ (°) | 90.00 |
| $\gamma$ (°) | 90.00 |
| Volume (Å$^3$) | 2835.10(11) |
| Z | 4 |
| Calculated density (g/cm$^{-3}$) | 1.291 |
| Absorption coefficient (mm$^{-1}$) | 0.728 |
| F(000) | 1088 |
| Reflections collected | 46265 |
| Independent reflections [*R*(int)] | 3348 [R(int) = 0.0323] |
| Refinement method | Full-matrix least-squares on $F^2$ |
| Data/restraints/parameters | 3348/0/224 |
| Goodness-of-fit on $F^2$ | 1.093 |
| Final *R* indices [$I > 2$sigma($I$)] | $R_1 = 0.0680$, $wR_2 = 0.2209$ |
| *R* indices (all data) | $R_1 = 0.0769$, $wR_2 = 0.2413$ |
| Largest difference peak and hole (e/Å$^3$) | 0.865 and -1.051 |

**Table S3**. Selected bond distances and angles of $[Fe^{II}(13\text{-TMC})(NCS)](CF_3SO_3)$.

| | | | |
|---|---|---|---|
| | Distances (Å) | | |
| Fe1-N1 | 2.172(3) | Fe1-N3 | 2.164(4) |
| Fe1-N2 | 2.204(2) | Fe1-N4 | 1.983(4) |
| Fe1-N2’ | 2.204(2) | | |
| | Angles (º) | | |
| N1 Fe1 N2 | 80.68(6) | N2 Fe1 N3 | 88.61(6) |
| N1 Fe1 N2’ | 80.68(6) | N2 Fe1 N4 | 104.88(6) |
| N1 Fe1 N3 | 136.89(14) | N2’ Fe1 N3 | 88.61(7) |
| N1 Fe1 N4 | 114.39(15) | N2’ Fe1 N4 | 104.86(6) |
| N2 Fe1 N2’ | 149.39(12) | N3 Fe1 N4 | 108.72(17) |

**Table S4**. DFT energies in kcal/mol.

| | Δlacvp | Δlacv3p$^{*+}$ | **ΔE**$^{a}$ | $\Delta Z_0$ | $\Delta E_{thermal}$$^{b}$ | -TΔS$^{b}$ | ΔDisp | **ΔG**$^{d}$ |
|---|---|---|---|---|---|---|---|---|
| No NCS (**$^{BH}$2**) | | | | | | | | |
| *S* = 1/2 | 10.00 | +6.36 | **16.36** | +2.01 | -0.54 | +2.23 | -4.46 | **15.61** |
| *S* = 3/2 | 4.19 | +5.09 | **9.28** | +1.01 | -0.18 | +0.82 | -3.45 | **7.48** |
| *S* = 5/2 | 0.00 | +0.00 | **0.00** | +0.00 | +0.00 | +0.00 | +0.00 | **0.00** |
| With NCS (**3**) | | | | | | | | |
| *S* = 1/2 | -4.44 | +4.83 | **0.38** | +3.18 | -0.97 | +3.76 | -0.11 | **6.24** |
| *S* = 3/2 | 9.21 | +3.92 | **13.13** | +1.33 | -0.39 | +1.66 | +1.85 | **17.58** |
| *S* = 5/2 | 0.00 | +0.00 | **0.00** | +0.00 | +0.00 | +0.00 | +0.00 | **0.00** |

[a] Sum of the two previous columns. [b] T = 233.15 K. [c] $\Delta G = \Delta E + \Delta Z_0 + \Delta E_{thermal}$ - TΔS + ΔDisp. This value is however not deemed to be reliable due to double counting of effects (see DFT methods section above).

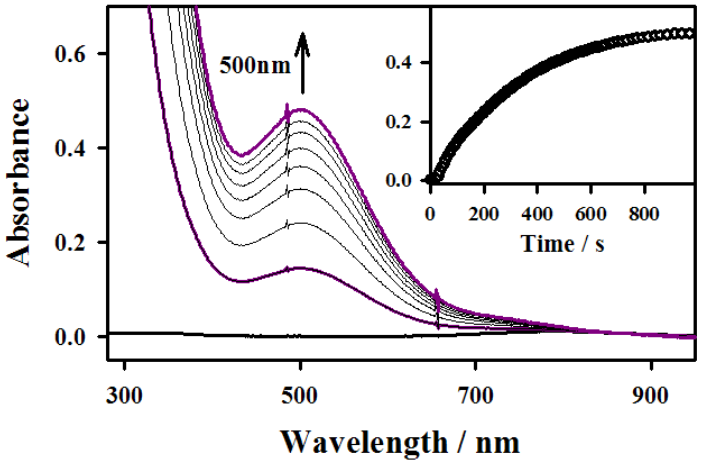


**Fig. S1** UV-vis spectral changes observed in the reaction of $Fe^{II}$(13-TMC)$(CF_3SO_3)_2$ (**1**; 0.50 mM) and Cumyl-OOH (1.5 mM) in $CH_3CN$ at –40 ºC. Inset shows time trace monitored at 510 nm due to $[Fe^{III}(OOC(CH_3)_2C_6H_5)(13\text{-TMC})]^{2+}$.

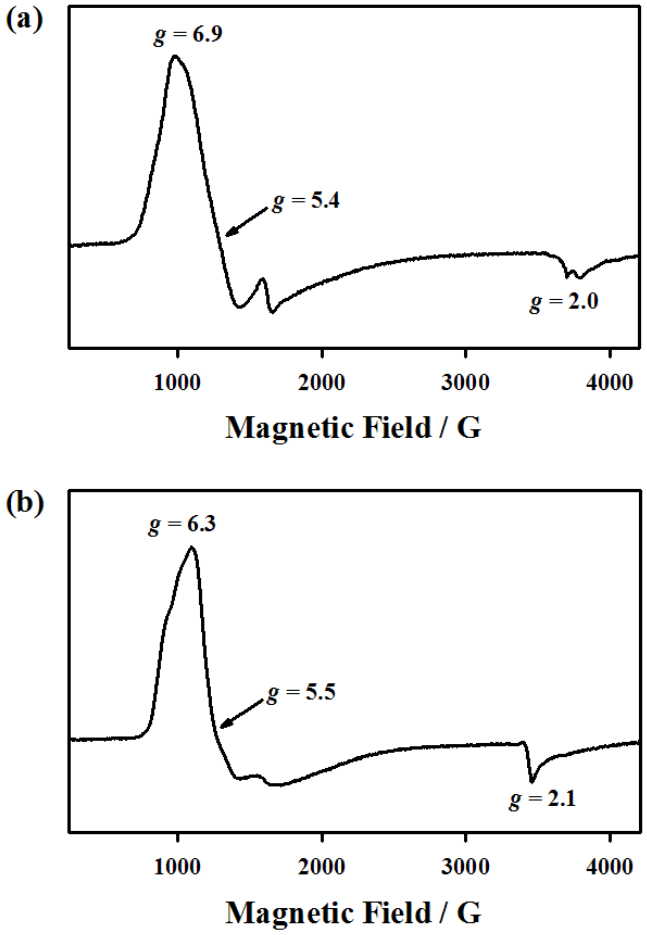


**Fig. S2** X-band EPR spectra of $^{BH}$**2** (a) and $^{CH}$**2** (b) recorded at 5.0 K. $^{BH}$**2** (a) and $^{CH}$**2** (b) were generated by reacting **1** (0.50 mM) with *t*-BuOOH (1.5 mM) and Cumyl-OOH (1.5 mM) in $CH_3CN$ at –40 °C, respectively. The experimental parameters for EPR measurements were as follows: Microwave frequency = 9.646 GHz, microwave power = 1.0 mW, modulation amplitude = 10 G, gain = 1.0 x $10^4$, modulation frequency = 100 kHz, time constant = 81.92 ms, and conversion time = 81.00 ms.

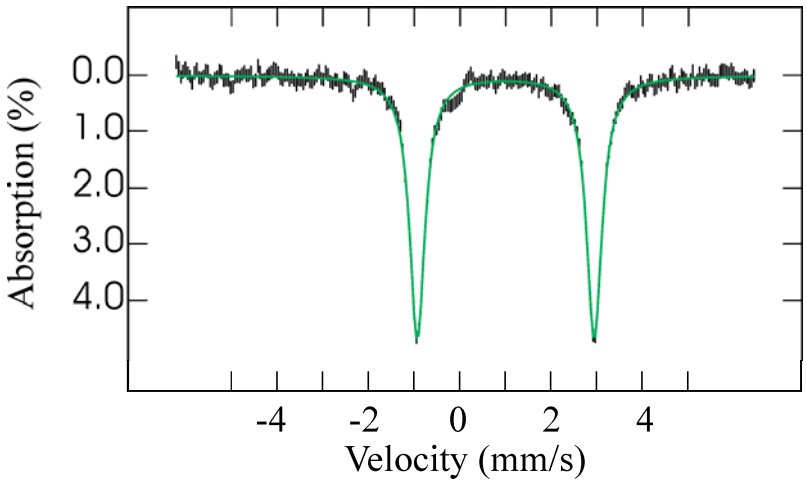


**Fig. S3** Mössbauer spectrum of **1** in acetonitrile measured at 4.2K in a 0.06 T applied magnetic field. Data points are represented with vertical bars, while the green line is a quadrupole doublet simulation with the parameters listed in Table S2.

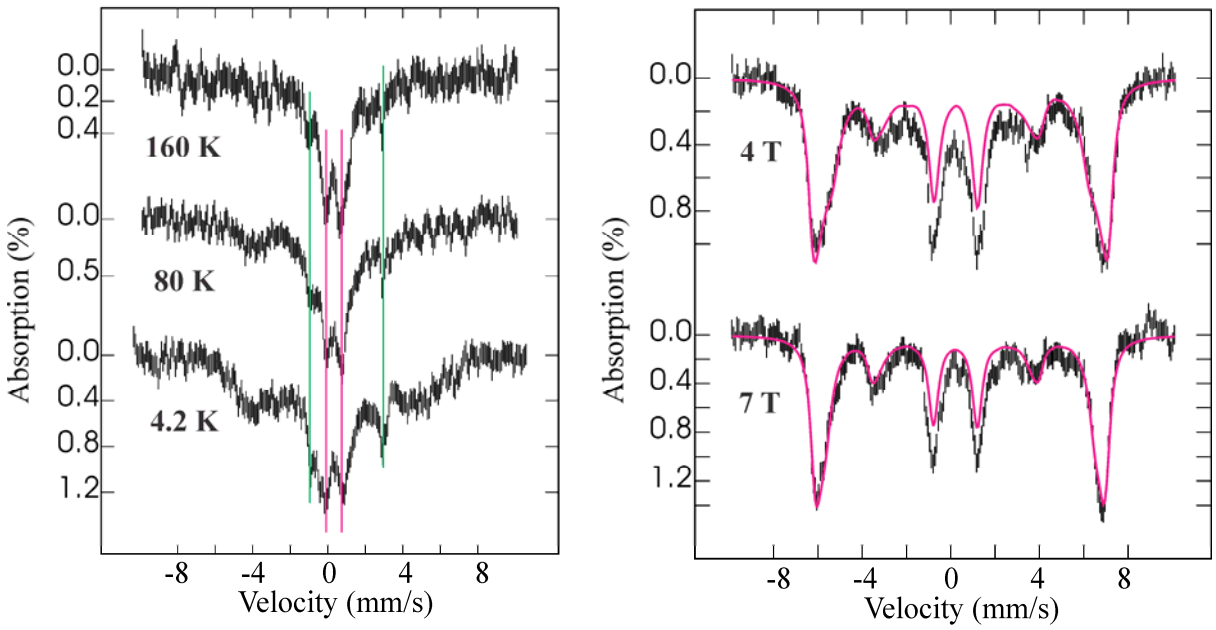


**Fig. S4** Mössbauer spectra of **1** + *t*-BuOOH measured at various temperatures in the absence of an applied magnetic field (left panel) or in a weak magnetic field of 600 G (left panel, 4.2 K spectrum), or at 4.2 K and in presence of a varying magnetic field applied parallel to the direction of the gamma-rays (right panel). On the left panel, unreacted **1** appears as a quadrupole doublet whose lines are indicated by green vertical bars (~8% of overall absorption). The central doublet indicated by pink vertical bars corresponds to high-spin $Fe^{III}$ with lower than normal isomer shift (see Table S1). Its intensity relative to that of the $Fe^{II}$ doublet increases with increasing temperature. Conversely, the area under the broad magnetic component decreases with increasing temperature, indicating that both $Fe^{III}$ components can be assigned to fractions of the same complex ($^{BH}$**2**) with different relaxation behaviors: Higher temperatures favor fast relaxation, causing most of the intensity to collapse under the central quadrupole doublet. On the right panel, strong applied magnetic fields make electronic relaxation slower; therefore the high-filed spectra were simulated in the slow-relaxation limit. The pink solid lines are spin-Hamiltonian simulations of the $S = 5/2$ ferric component with parameters listed in Table S1.

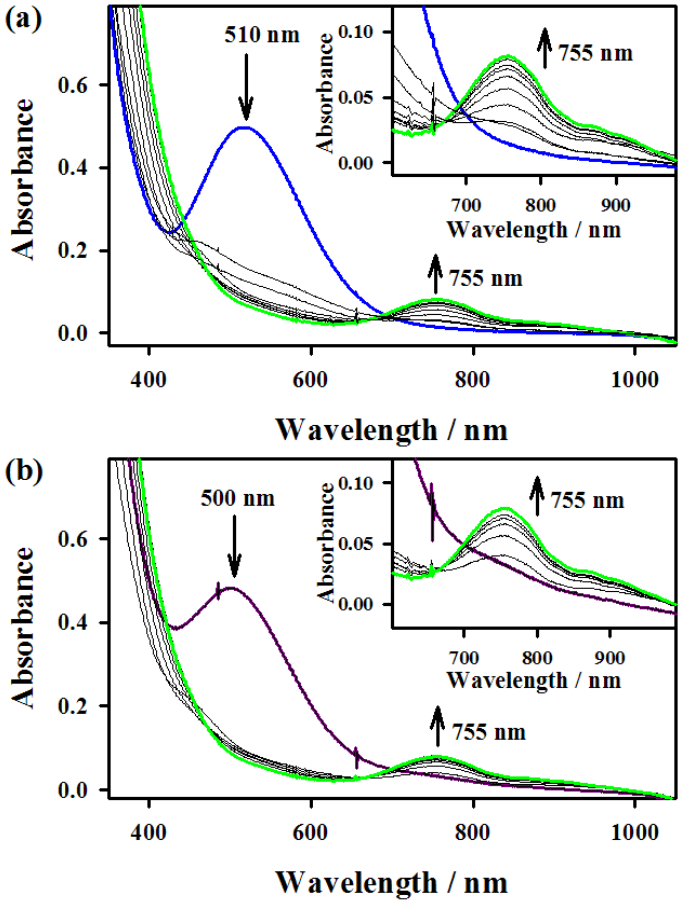


**Fig. S5** UV-vis spectral changes observed in the conversion of $^{BH}$**2** (a, 0.50 mM; blue line) and $^{CH}$**2** (b, 0.50 mM; purple line) to **4** (green line) in $CH_3CN$ at –40 ºC.

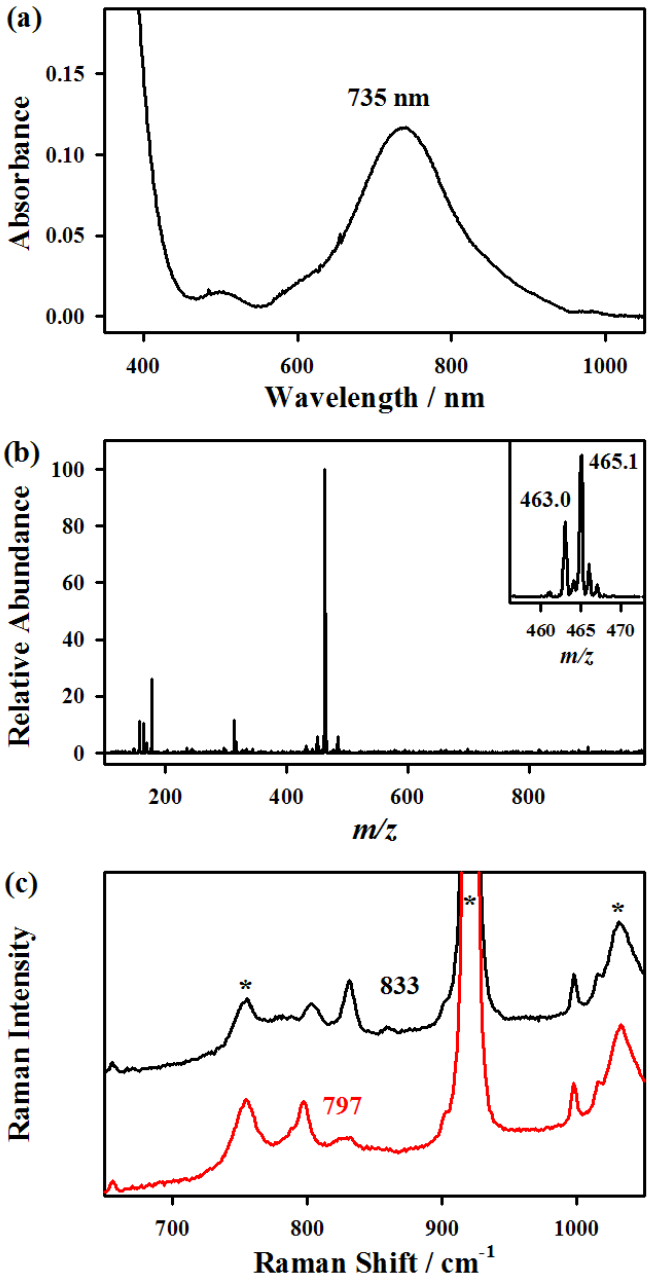


**Fig. S6** (a) UV-vis spectrum of **6** (0.50 mM) in $CH_3CN$ at –40 °C. (b) ESI MS spectrum of **6** in $CH_3CN$ at –40 °C. Inset shows the prominent ion peaks at *m/z* 463.0 and 465.1, whose mass and isotope distribution patterns correspond to $[Fe^{IV}(^{16}O)(13\text{-TMC})(CF_3SO_3)]^+$ (calculated *m/z* 463.1; **6**-$^{16}$O) and $[Fe^{IV}(^{16}O)(13\text{-TMC})(CF_3SO_3)]^+$ (calculated *m/z* 465.1; **6**-$^{18}$O), respectively.[S3] (c) rRaman spectra of **6**-$^{16}$O (black) and **6**-$^{18}$O (red) upon 407 nm excitation in $CH_3CN$ at –40 °C.[S3] The peaks marked with * are from solvent.

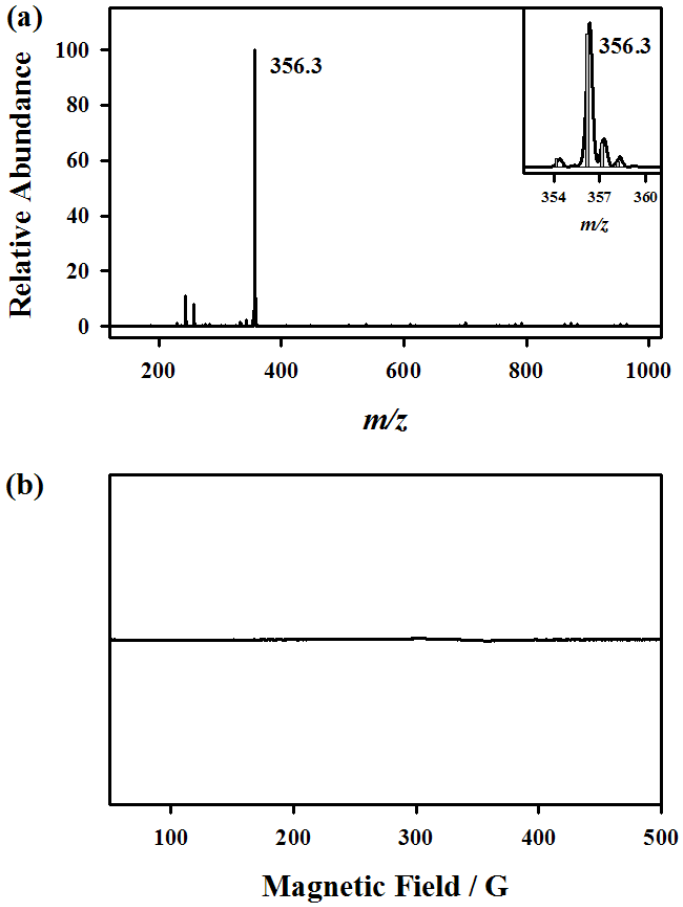


**Fig. S7** (a) ESI-MS spectrum of $[Fe^{II}(13\text{-TMC})(NCS)](CF_3SO_3)$ in $CH_3CN$ at room temperature. One prominent peak at *m/z* of 356.3 corresponds to $[Fe^{II}(13\text{-TMC})(NCS)]^+$ (calculated *m/z* 356.2). Inset shows the isotopic distributions of the peak. (b) X-band EPR spectrum of $[Fe^{II}(13\text{-TMC})(NCS)](CF_3SO_3)$ (1.0 mM) recorded at 5.0 K. The experimental parameters for EPR spectra are as follows: Microwave frequency = 9.646 GHz, microwave power = 1.0 mW, modulation amplitude = 10 G, gain = 1.0 x $10^4$ and modulation frequency 100 kHz.

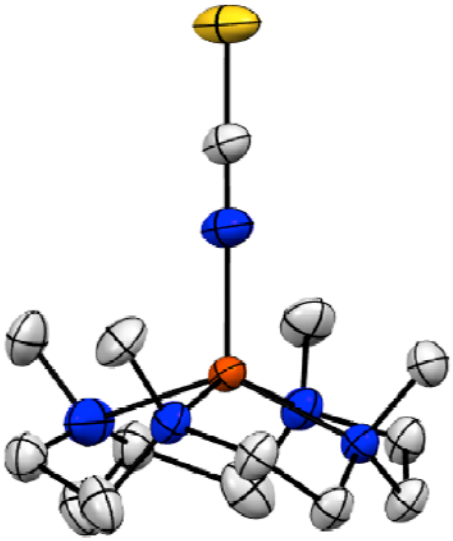

**Fig. S8** ORTEP diagram of $[Fe^{II}(13\text{-TMC})(NCS)]^{+}$ moiety in the molecular structure of $[Fe^{II}(13\text{-TMC})(NCS)](CF_3SO_3)$ with 50% probability ellipsoids. H atoms are omitted for clarity.

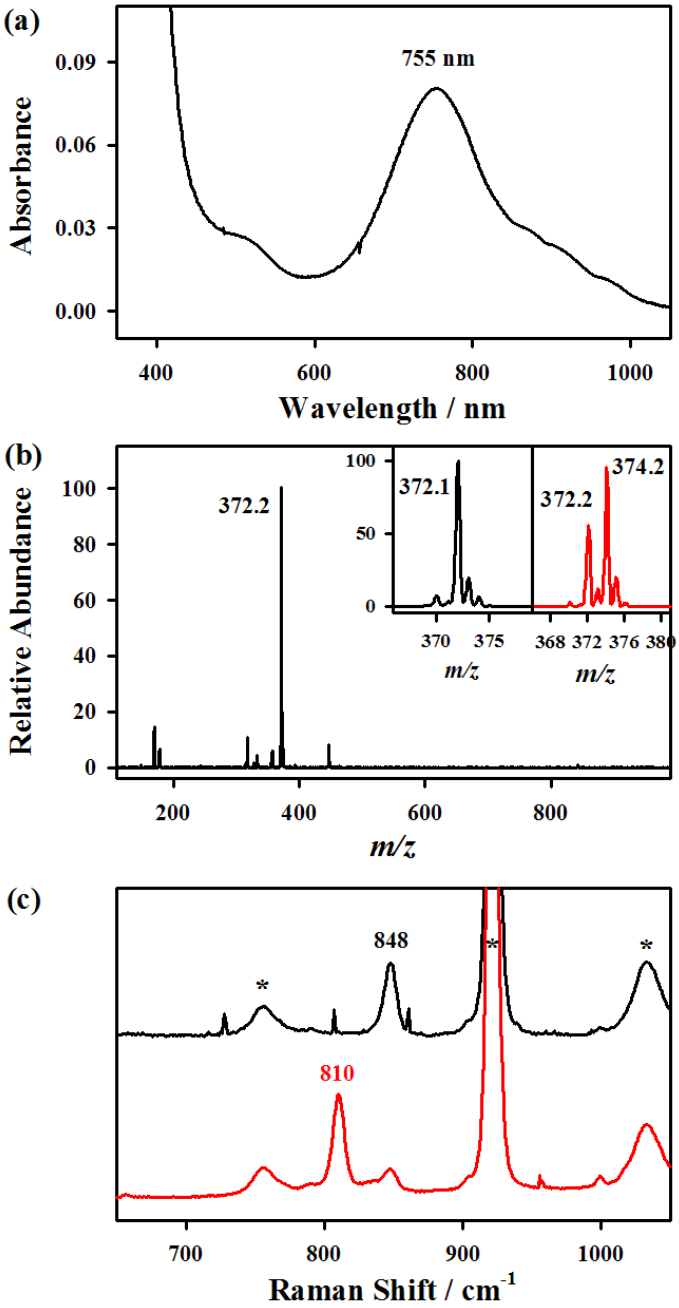


**Fig. S9** (a) UV-vis spectrum of **4** (0.50 mM) in $CH_3CN$ at –40 °C. (b) ESI MS spectrum of **4** in $CH_3CN$ at –40 °C. Inset shows ESI MS spectra of **4**-$^{16}O$ (left panel) and **4**-$^{18}O$ (right panel). The mass and isotope distribution patterns of the peaks at *m/z* 372.2 and 374.2 correspond to $[Fe^{IV}(^{16}O)(13\text{-TMC})(NCS)]^+$ (calculated *m/z* 372.2) and $[Fe^{IV}(^{18}O)(13\text{-TMC})(NCS)]^+$ (calculated *m/z* 374.2), respectively. (c) rRaman spectra of **4**-$^{16}O$ (black line) and **4**-$^{18}O$ (red line) in $CH_3CN$ at –40 °C upon 407-nm excitation. The peaks marked with * are from solvent.

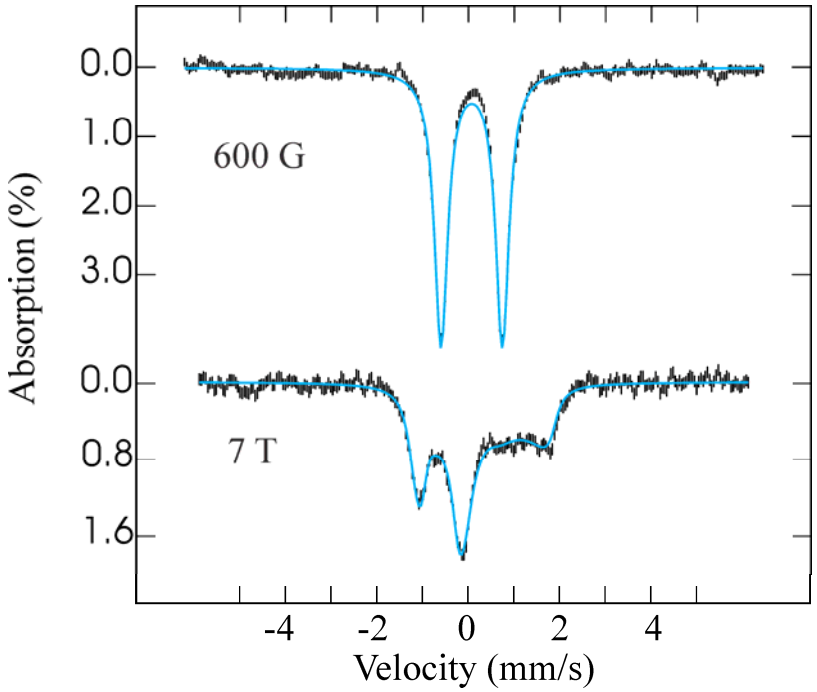


**Fig. S10** Mössbauer spectra of genuine **4** recorded at 4.2 K in a magnetic field of 0.06 T or 7 T applied parallel to the direction of the γ–rays. The blue solid lines are spin-Hamiltonian simulations using parameters listen in Table S1 for **4**.

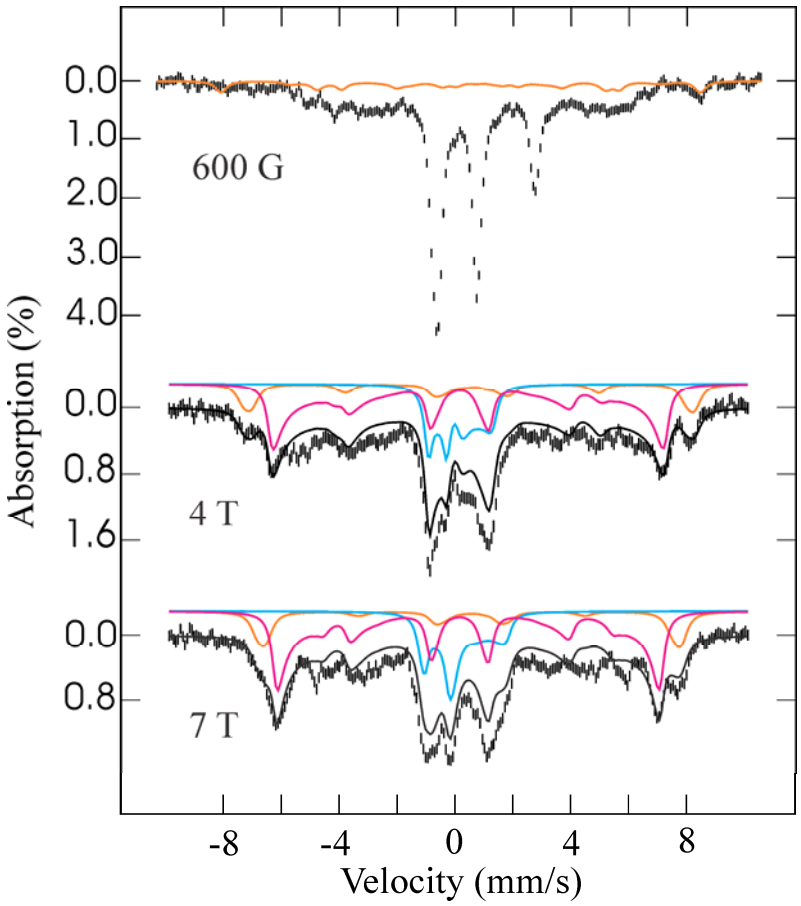


**Fig. S11** Variable field Mössbauer spectra of **1** + $^{t}$BuOOH after $NCS^{-}$ addition at –40°C. Data was collected at 4.2 K in varying magnetic fields applied parallel to the γ–rays. The 600 G spectrum shows two prominent doublets as described in the text, assigned to an $Fe^{II}$ and an $Fe^{IV}$=O species. The 4 T and 7 T spectra display spin-Hamiltonian simulations with an $S = 1$ component accounting for the $Fe^{IV}$=O complex (blue lines, 20% of total absorption), and two $S = 5/2$ components representing each a high-spin $Fe^{III}$ complex (orange and pink lines). The orange component accounts for only 13% of total iron and has parameters typical for octahedral high-spin $Fe^{III}$. Its simulation is also shown in the 600 G spectrum. The pink component, in contrast, accounts for 42% of total iron and behaves very similarly to the complex assigned to $^{BH}$**2**, with an unresolved spectrum in low-field and parameters that are uncommon for octahedral high-spin $Fe^{III}$ (low isomer shift and large zero-field splitting). The black solid lines are composite theoretical spectra obtained by combining the individual contributions. They do not contain contributions from the $S = 2$ ferrous complex, which was not simulated in high-field. All parameters used in the simulations are listed in Table S1.

## DFT Optimized Coordinates

Coordinates for $^{BH}$**2** and **3** are given in xyz-file format, with the (charge/multiplicity) given in the comment line.

```
63
BH2 (2/2)
Fe -0.10932 -1.94200 2.32086
N 1.94332 -2.13326 2.52877
N 0.28628 -0.13416 1.33077
N -2.15854 -1.58301 2.57370
N -0.22107 -3.19580 3.94046
C -0.12555 -0.10479 -0.11498
C 1.79764 0.05686 1.40646
C 2.36701 -0.68045 2.60587
C 2.70105 -2.81589 1.41916
O -0.44069 -2.96475 0.90661
O 0.26976 -4.28622 0.80073
C -0.17478 -5.01126 -0.44752
C 0.17261 -4.17125 -1.67809
C -0.35994 1.00875 2.10352
C -1.87953 0.94029 2.23688
C -2.39673 -0.18889 3.12527
C -3.01538 -1.80177 1.35625
C 1.00083 -2.79347 4.73923
C 2.22209 -2.85791 3.83653
C -0.22971 -4.67497 3.67355
C -1.49647 -2.79581 4.65176
C -2.58592 -2.60824 3.61486
C 0.68789 -6.27911 -0.35138
C -1.66798 -5.33251 -0.35401
H -0.21333 -5.20817 4.63034
H -1.12721 -4.94040 3.11888
H 0.62567 -4.95493 3.06756
H -2.82086 -2.79624 0.96417
H -4.07120 -1.70630 1.63479
H -2.78770 -1.07029 0.58642
H 0.19860 0.83701 -0.57256
H 0.33218 -0.94698 -0.63157
H -1.20462 -0.18859 -0.20490
H 2.02830 1.12555 1.46502
H 2.23042 -0.31570 0.47824
H 2.46902 -2.35580 0.46120
H 3.77578 -2.73244 1.61646
H 2.39990 -3.85694 1.37069
H 1.99592 -0.26020 3.54615
H 3.46089 -0.61369 2.62156
H 3.09414 -2.41550 4.32915
H 2.47317 -3.89079 3.59387
H -1.77574 -3.56622 5.37823
H -1.30661 -1.87396 5.20621
H -3.52310 -2.28627 4.08300
H -2.78270 -3.54238 3.08625
H -1.91428 -0.13068 4.10522
H -3.47704 -0.07665 3.28196
H -2.19162 1.87939 2.71045
H -2.36718 0.93688 1.25744
H 0.09799 1.02583 3.09805
H -0.07892 1.93906 1.59378
H 0.83380 -1.77715 5.10882
H 1.11914 -3.44885 5.60948
H -0.07323 -4.72964 -2.58777
H -0.39586 -3.23758 -1.68550
H 1.24157 -3.93678 -1.69599
H -1.95663 -5.98721 -1.18331
H -1.89321 -5.84766 0.58498
H -2.27221 -4.42413 -0.41563
H 0.47147 -6.92448 -1.20910
H 1.75301 -6.02989 -0.36675
H 0.46542 -6.83542 0.56416

63
BH2 (2/4)
Fe -0.07859 -2.04943 2.21197
N 1.98733 -2.15436 2.43568
N 0.28778 -0.18987 1.26571
N -2.09883 -1.66354 2.63236
N -0.10550 -3.17583 3.95882
C -0.19548 -0.17125 -0.16153
C 1.79995 -0.00065 1.25619
C 2.42903 -0.70787 2.43896
C 2.64327 -2.91523 1.31117
O -0.34229 -3.10924 0.67540
O 0.04110 -4.55057 0.66477
C -0.28096 -5.16890 -0.67308
C 0.52489 -4.46641 -1.76692
C -0.32730 0.95123 2.05699
C -1.83828 0.86718 2.26232
C -2.30308 -0.26073 3.18024
C -2.99835 -1.89940 1.44669
C 1.13938 -2.74614 4.70122
C 2.32418 -2.83353 3.75651
C -0.08729 -4.65412 3.67218
C -1.36167 -2.81159 4.71292
C -2.48577 -2.66828 3.70875
C 0.19520 -6.60977 -0.43744
C -1.78991 -5.09383 -0.91218
H -0.00086 -5.19800 4.61919
H -1.00557 -4.94082 3.16456
H 0.74083 -4.91005 3.01755
H -2.81833 -2.90001 1.06072
H -4.04330 -1.79559 1.76064
H -2.79462 -1.17841 0.66027
H 0.13432 0.75472 -0.64637
H 0.21118 -1.03452 -0.68574
H -1.27999 -0.21901 -0.19937
H 2.03377 1.06896 1.27430
H 2.18016 -0.39736 0.31464
H 2.46064 -2.41953 0.36099
H 3.72164 -2.96902 1.49612
H 2.21437 -3.91384 1.25774
H 2.11284 -0.26002 3.38508
H 3.52297 -0.65568 2.38986
H 3.21078 -2.36414 4.19466
H 2.57885 -3.87120 3.53957
H -1.59276 -3.58319 5.45530
H -1.17797 -1.87897 5.24983
H -3.41403 -2.34377 4.19223
H -2.68726 -3.61684 3.20828
H -1.77322 -0.19638 4.13370
H -3.37510 -0.14978 3.38696
H -2.13711 1.80436 2.74793
H -2.37370 0.85660 1.30825
H 0.17627 0.98052 3.02805
H -0.08299 1.88008 1.52573
H 0.98147 -1.72084 5.04683
H 1.29149 -3.37897 5.58361
H 0.34248 -4.95099 -2.73218
H 0.23207 -3.41633 -1.84881
H 1.59678 -4.52000 -1.55177
H -2.04865 -5.62692 -1.83336
H -2.33347 -5.55649 -0.08196
H -2.11453 -4.05508 -1.01440
H 0.02418 -7.19951 -1.34403
H 1.26448 -6.63419 -0.20620
H -0.35719 -7.07299 0.38573

63
BH2 (2/6
Fe -0.18317 -2.05030 2.12062
N 2.00587 -2.09461 2.52086
N 0.25806 -0.06025 1.29498
N -2.26832 -1.59253 2.67576
N -0.18539 -3.11284 4.04592
C -0.19020 0.07366 -0.13847
C 1.76863 0.08790 1.34440
C 2.37425 -0.63372 2.53976
C 2.75705 -2.83595 1.45044
O -0.36203 -3.23291 0.69576
O 0.09244 -4.62359 0.67922
C -0.18553 -5.25132 -0.68197
C 0.61290 -4.49553 -1.74326
C -0.37516 1.02167 2.15125
C -1.89542 0.93272 2.31382
C -2.40423 -0.18697 3.22518
C -3.22039 -1.80436 1.52823
C 1.03897 -2.60875 4.76420
C 2.25989 -2.73826 3.86409
C -0.13757 -4.59956 3.83165
C -1.45276 -2.72400 4.76051
C -2.59628 -2.59318 3.76391
C 0.34601 -6.66914 -0.44177
C -1.69262 -5.22354 -0.93298
H -0.00375 -5.10605 4.79480
H -1.06890 -4.93206 3.37426
H 0.67456 -4.86700 3.15860
H -3.10588 -2.82072 1.15201
H -4.25249 -1.64772 1.86450
H -3.00241 -1.10548 0.72183
H 0.11073 1.05094 -0.53345
H 0.26543 -0.71821 -0.73375
H -1.27245 -0.01784 -0.20815
H 2.02729 1.15277 1.37886
H 2.16841 -0.31097 0.41101
H 2.60705 -2.36063 0.48248
H 3.82850 -2.84606 1.68451
H 2.38036 -3.85655 1.38919
H 2.01132 -0.20691 3.47870
H 3.46623 -0.52502 2.52598
H 3.13293 -2.27866 4.34157
H 2.50439 -3.78728 3.68978
H -1.70091 -3.47531 5.51921
H -1.27185 -1.78269 5.28258
H -3.51575 -2.28761 4.27903
H -2.79501 -3.54974 3.27549
H -1.86371 -0.14646 4.17362
H -3.46820 -0.02360 3.44504
H -2.20539 1.87298 2.78696
H -2.40244 0.92319 1.34410
H 0.10155 0.98183 3.13547
H -0.11484 1.98676 1.69583
H -0.85806 -1.56347 5.02986
H 1.19189 -3.16998 5.69490
H 0.46213 -4.96560 -2.72080
H 0.28353 -3.45504 -1.80829
H 1.68229 -4.51664 -1.51201
H -1.91930 -5.74319 -1.86983
H -2.22849 -5.72543 -0.12134
H -2.05378 -4.19500 -1.01519
H 0.21587 -7.25729 -1.35600
H 1.41101 -6.65112 -0.19210
H -0.20266 -7.16132 0.36659

66
3 (1/2)
Fe -0.01895 -1.85042 2.51715
N 2.00844 -2.10147 2.51325
N 0.30318 -0.15961 1.29330
N -2.10424 -1.62890 2.75249
N -0.08451 -3.25131 4.02914
C 0.01165 -0.38032 -0.16778
C 1.80375 0.14825 1.43752
C 2.53230 -0.68324 2.50851
C 2.58077 -2.81017 1.31204
O -0.31956 -2.83435 1.01647
O 0.03744 -4.30448 0.93445
C -0.25430 -4.84614 -0.43587
C 0.60439 -4.14618 -1.49371
C -0.51524 1.03630 1.75699
C -2.02263 0.78901 1.90281
C -2.48498 -0.18271 2.99856
C -2.91356 -2.13620 1.58779
C 1.23168 -3.05139 4.75391
C 2.38250 -2.90662 3.75205
C -0.24097 -4.70509 3.68048
C -1.27440 -2.81572 4.86174
C -2.46252 -2.50386 3.95489
C 0.16640 -6.31411 -0.25302
C -1.74875 -4.72672 -0.74706
H -0.31070 -5.28541 4.60854
H -1.13522 -4.85315 3.08059
H 0.60947 -5.04050 3.09468
H -2.67635 -3.18040 1.41505
H -3.98120 -2.02320 1.81498
H -2.67709 -1.57916 0.68561
H 0.25901 0.52779 -0.73091
H 0.59847 -1.21612 -0.53517
H -1.04054 -0.61562 -0.31076
H 1.92992 1.21158 1.66202
H 2.26157 -0.02500 0.46194
H 2.36737 -2.24514 0.40798
H 3.66664 -2.89624 1.43619
H 2.12220 -3.78964 1.22107
H 2.40609 -0.26392 3.50043
H 3.60572 -0.69633 2.27897
H 3.24986 -2.45053 4.24094
H 2.69106 -3.89291 3.40031
H -1.55142 -3.61829 5.55662
H -0.98657 -1.94945 5.44956
H -3.25674 -2.01982 4.53434
H -2.87480 -3.43311 3.55745
H -2.08468 0.11004 3.96661
H -3.58140 -0.14028 3.06378
```

```
H -2.46488 1.76313 2.15132
H -2.46257 0.51530 0.93813
H -0.09819 1.37856 2.70020
H -0.36270 1.83634 1.01890
H 1.14525 -2.16982 5.38087
H 1.42621 -3.91129 5.40670
H 0.44736 -4.62209 -2.46809
H 0.33136 -3.09239 -1.58506
H 1.66755 -4.21941 -1.24631
H -1.96969 -5.22473 -1.69767
H -2.34505 -5.20536 0.03662
H -2.04693 -3.67932 -0.83250
H 0.00862 -6.85666 -1.19122
H 1.22541 -6.38587 0.01352
H -0.42905 -6.79425 0.52931
N 0.19897 -0.53482 4.02831
C 0.32601 0.24900 4.91511
S 0.49496 1.32354 6.13141

66
3 (1/4)
Fe -0.05968 -1.86932 2.47003
N 1.98097 -2.16095 2.51555
N 0.43917 -0.07626 1.29177
N -2.11999 -1.56146 2.69463
N -0.18438 -3.27400 4.12689
C 0.21159 -0.33946 -0.17052
C 1.92512 0.16406 1.54550
C 2.53651 -0.75131 2.62279
C 2.62750 -2.81424 1.31991
O -0.54361 -3.08496 1.09282
O 0.23012 -4.34188 0.78862
C -0.24271 -4.94575 -0.50166
C -0.01999 -3.96332 -1.65418
C -0.38980 1.11505 1.72229
C -1.90411 0.86406 1.81490
C -2.42075 -0.08287 2.91285
C -2.95622 -2.04027 1.53723
C 1.15014 -3.07257 4.79049
C 2.27068 -3.03494 3.74066
C -0.38966 -4.71025 3.76191
C -1.36882 -2.74270 4.88564
C -2.51448 -2.39981 3.92334
C 0.68320 -6.16817 -0.60549
C -1.71042 -5.36459 -0.37308
H -0.39367 -5.32523 4.67156
H -1.33754 -4.82868 3.23906
H 0.39489 -5.04547 3.08749
H -2.75777 -3.09204 1.36364
H -4.01490 -1.88347 1.77516
H -2.70433 -1.48868 0.63440
H 0.54350 0.52134 -0.76517
H 0.75649 -1.23005 -0.47490
H -0.84699 -0.51310 -0.35633
H 2.07958 1.20585 1.84209
H 2.44770 0.02736 0.59598
H 2.52309 -2.17621 0.44457
H 3.69362 -2.95239 1.53409
H 2.14176 -3.76298 1.11854
H 2.33656 -0.38212 3.62111
H 3.62346 -0.79883 2.48089
H 3.20530 -2.69730 4.20174
H 2.44128 -4.04068 3.35268
H -1.73478 -3.49499 5.59827
H -1.05473 -1.87069 5.45102
H -3.30587 -1.87139 4.46645
H -2.94899 -3.32062 3.53119
H -2.02168 0.19788 3.88277
H -3.51461 0.00448 2.95729
H -2.35556 1.84143 2.03157
H -2.30838 0.57739 0.83857
H -0.00944 1.44847 2.68503
H -0.21562 1.92211 0.99553
H 1.11461 -2.14844 5.35973
H 1.36014 -3.89418 5.48899
H -0.30073 -4.43227 -2.60367
H -0.62973 -3.06700 -1.51842
H 1.03338 -3.67073 -1.71376
H -2.01744 -5.92342 -1.26414
H -1.85060 -6.00726 0.50208
H -2.36048 -4.49163 -0.27888
H 0.44194 -6.73144 -1.51321
H 1.73196 -5.86028 -0.65881
H 0.55147 -6.82949 0.25649
N 0.17607 -0.42170 4.14772
C 0.30357 0.36261 5.03681
S 0.47428 1.43932 6.25836

66
3 (1/6)
Fe -0.06757 -1.87127 2.43764
N 2.10784 -2.11113 2.54669
N 0.36878 -0.09840 1.26461
N -2.20826 -1.66102 2.80306
N -0.06842 -3.23288 4.14130
C 0.13363 -0.32741 -0.20601
C 1.85648 0.18725 1.49473
C 2.56152 -0.67497 2.57336
C 2.70557 -2.81383 1.36246
O -0.32019 -2.99926 0.92345
O -0.00064 -4.43070 0.78822
C -0.31009 -4.93555 -0.60617
C 0.55041 -4.18854 -1.62572
C -0.51804 1.05091 1.72422
C -2.02479 0.73114 1.84490
C -2.52542 -0.18809 2.98318
C -3.04806 -2.21203 1.68273
C 1.25684 -2.97874 4.81779
C 2.41454 -2.90365 3.80300
C -0.20890 -4.68012 3.78116
C -1.25825 -2.76401 4.94519
C -2.48358 -2.48483 4.05537
C 0.10699 -6.40599 -0.46447
C -1.80663 -4.78449 -0.87912
H -0.20396 -5.28970 4.69381
H -1.14031 -4.84320 3.24063
H 0.60844 -4.98500 3.13061
H -2.80699 -3.26187 1.53375
H -4.11276 -2.10364 1.92650
H -2.83786 -1.68026 0.75645
H 0.39477 0.57691 -0.76938
H 0.73883 -1.16269 -0.54973
H -0.91350 -0.56875 -0.38500
H 1.97817 1.24095 1.76460
H 2.35651 0.04759 0.53366
H 2.51283 -2.24392 0.45463
H 3.79051 -2.91268 1.49565
H 2.24969 -3.79605 1.25298
H 2.37193 -0.28257 3.56662
H 3.64397 -0.62900 2.38783
H 3.30048 -2.49110 4.30025
H 2.67365 -3.91241 3.47361
H -1.53555 -3.53273 5.67902
H -0.96438 -1.87108 5.48886
H -3.25304 -1.98716 4.65788
H -2.90813 -3.43221 3.71616
H -2.10978 0.12734 3.93734
H -3.61951 -0.09350 3.04232
H -2.51076 1.70106 2.01610
H -2.41728 0.38826 0.88142
H -0.13216 1.40426 2.67619
H -0.40094 1.86218 0.99163
H 1.17383 -2.05134 5.37643
H 1.47115 -3.78673 5.53020
H 0.39801 -4.61845 -2.62157
H 0.27661 -3.13140 -1.66561
H 1.61193 -4.27278 -1.37396
H -2.05100 -5.22776 -1.85045
H -2.39312 -5.29727 -0.11001
H -2.09223 -3.72999 -0.90104
H -0.06080 -6.92179 -1.41565
H 1.16796 -6.48815 -0.20977
H -0.48394 -6.90600 0.30874
N 0.17374 -0.36755 4.14437
C 0.29836 0.42797 5.02456
S 0.46410 1.51934 6.23429
```